Functional adaptation of bone mechanical properties using a diffusive stimulus originated by dynamic loads in bone remodelling

Rachele Allena

rachele.allena@univ-cotedazur.fr

Université Côte d'Azur

Daria Scerrato

Sapienza University of Rome

Alberto Bersani

Sapienza University of Rome

Ivan Giorgio

University of L'Aquila

Research Article

Keywords: Bone remodelling, Fick's laws of diffusion, Fourier's laws of diffusion, bio-mechanical stimulus, Growth Mechanics.

Posted Date: January 11th, 2024

DOI: https://doi.org/10.21203/rs.3.rs-3845178/v1

Additional Declarations: No competing interests reported.

Version of Record: A version of this preprint was published at Zeitschrift für angewandte Mathematik und Physik on April 21st, 2024. See the published version at https://doi.org/10.1007/s00033-024-02230-x.

Functional adaptation of bone mechanical properties using a diffusive stimulus originated by dynamic loads in bone remodelling

Rachele Allena, Daria Scerrato, Alberto M. Bersani and Ivan Giorgio

Abstract. The present study proposes a mathematical model elucidating some aspects of the bio-mechanical stimulus involved in bone remodelling, which, in our assumptions, acts as a diffusive signalling agent for bones. The proposed mathematical model aims to scrutinize the behaviour of bone tissues and their evolution over time by better understanding the mechanisms of bone remodelling and offering new theoretical tools for developing more effective and efficient treatment strategies for bone defects, trauma, or diseases. The bone remodelling process involves adapting bone mechanical properties in response to dynamic loads. This adaptation is achieved through the diffusive stimulus created by these loads. The result is a functional adaptation of the bone, wherein it acquires the mechanical properties required to withstand the loads to which it is subjected. This phenomenon has significant implications for the study of bone physiology and biomechanics. As such, it is a topic of great interest to researchers and practitioners in the fields of orthopaedics, sports medicine, and related disciplines. In this contribution, the mechanical behaviour is modelled through a generalized three-dimensional deformable continuum that also takes into account the porous nature of the bone tissue with a nonlinear constitutive law. Since we have focused the study on the model of the stimulus and its interplay with the evolution of the tissue, an isotropic material symmetry is adopted to simplify the problem. This formulation is promising because it permits the bone tissue to evolve depending on the time-variability of the external mechanical loads, even if the source of the stimulus is assumed to be the strain energy density.

Mathematics Subject Classification (2010). 74L15 Biomechanical solid mechanics.

Keywords. Bone remodelling, Fick's laws of diffusion, Fourier's laws of diffusion, bio-mechanical stimulus, Growth Mechanics.

1. Introduction

The bone remodelling process is a lifelong process where aged or damaged bone tissue is removed from the skeleton —a process called bone resorption— and new bone tissue is formed —a process called ossification or new bone formation— ensuring turnover and renewal of bone tissues. Therefore, it is essential for maintaining the structural integrity and function of bones and allowing the body to adapt to changing mechanical and physiological demands. This process involves three main types of cells: *osteoclasts*, which break down old bone; *osteoblasts*, which form new bone; and *osteocytes*, which acquire information about the mechanical state of the tissue and activate the other two kinds of cells. Bone remodelling serves several purposes: i) it helps to maintain normal calcium levels in the body; ii) it allows the bone tissue to alter its strength and the architecture of its microstructure to optimize bone functionality in response to external mechanical requests; iii) it helps repair micro-damage to bones from everyday activity.

Modelling bone remodelling is still a major challenge due to the complexity of the phenomenon. In fact, it is regulated by biological, chemical and mechanical phenomena, which are still poorly understood [1,2]. Bones respond to mechanical forces by adapting their structure and density through a process known as *mechanotransduction*. When bones are subjected to dynamic loads, such as those experienced during physical activity or exercise, they experience mechanical strain. In response to this strain, bone cells are stimulated to initiate the remodelling process, leading to the formation of new bone tissue in areas that experience increased load and the removal of old or damaged tissue in the regions that experience reduced load. For instance, when a person engages in weight-bearing exercises or activities that involve impact and muscle contractions, the bones experience dynamic loading. This triggers a signalling cascade that involves various biochemical factors, leading to the activation of osteoclasts for bone resorption and osteoblasts for bone formation. In essence, dynamic loads play a crucial role in the bone remodelling process, helping to shape our bones and keep them strong and healthy [3–6]. On the contrary, this process is less responsive to static loads. Indeed, upon the application of a new constant load, the process undergoes an initial period of adjustment. However, after a certain amount of time, the process becomes acclimated to the new load and reaches a state of equilibrium. At this point, the evolution of the process stabilizes and is no longer subject to significant changes. It is important to note that this stabilization only occurs when the new load is constant, which allows the process to adapt and establish a new baseline.

During the last decades, several continuum models have been proposed to decipher the interactions between the different physics driving bone reconstruction [7–13]. Most of these works assume that the biological stimulus initiating bone remodelling does not spread but it maintains its local production site. Successive works have hypothesized that the stimulus in a material particle depends on a space average of the deformation in its neighbourhood. While these approaches are more realistic, it is still not clear how the stimulus forms, propagates and is perceived. Additionally, several microscale processes, such as the interstitial fluid flow across the lacuno-canalicular network, may play a critical role in the stimulus generation and activity [14, 15]. However, it is unequivocal that the stimulus is originated by biochemical processes, which facilitate the production of factors that diffuse within the bone [16, 17]. Then, our main objective is to formulate a model that is valid at the macroscale and accounts for the diffusion of biological stimulus during the process of bone remodelling. The stimulus is considered a macroscopic source of canalicular flow, representing the mechanical state of the tissue, and may influence the cellular behaviour over time [18–20].

The present study introduces a generalized three-dimensional deformable continuum model to simulate the mechanical behaviour of bone tissue. The model incorporates the porous nature of bone tissue (see, for more details about the model of this aspect, [21–30]) and employs a nonlinear constitutive law to simulate the mechanical response. The nonlinear behaviour is adopted in the formulation because, during the evolution, the stiffness of the bone can become very small in specific regions where negligible deformation occurs, allowing large displacement and deformations. To simplify the problem, we have adopted an isotropic material symmetry. In this way, we can deal solely with the evolution of one material parameter instead of many. Since this aspect is easily generalisable, as demonstrated in previous work (e.g., [31]), the results obtained with the present formulation are likewise generalizable. Our main focus has been to investigate the interaction between external mechanical loads and the evolution of bone tissue. We have assumed that the source of the stimulus for tissue evolution is the strain energy density, as in many previous works [32–34]. Two main improvements have to be noticed with respect to our previous work [35]. First, to be more realistic, we consider a three-dimensional (3D) geometry here, which mimics femoral diaphysis. Second, the external action is represented by a dynamic cyclic torsion characterized by different frequencies to mimic the physiological load the bone structure is subjected to.

The basic model employed for the stimulus in this contribution, given in prior works [32, 35, 36], is an improvement of the theory formulated by T. Lekszycki and F. dell'Isola [37] in the continuum context refining a former idea proposed by M. G. Mullender and R. Huiskes [38] in a discrete approach based on zones of influence of the osteocytes. However, the model proposed in [37], based

on a space convolution without a direct time dependence, considers that the signal stemming from the osteocytes in a given material particle of the bone was instantaneously transmitted throughout the bone tissue. This assumption implies that if the stimulus source is not time-dependent, like the strain energy density, the evolution is not affected by the time variability of the external loads, as demonstrated in [34]. In that case, the only way to consider the time dependence of the stimulus is to add a source which is time-dependent as, for example, dissipated energy [39]. As shown with the numerical simulations performed here, the proposed formulation, instead based on a diffusion equation governing the evolution of the stimulus, enables bone tissue to evolve based on the time-variability of external mechanical loads, also considering the strain energy density as a source that generates the bio-mechanical stimulus. This is because the stimulus is not instantaneously transmitted within the tissue as in [37], but it has a response that depends on the time due to the diffusion phenomenon. The results obtained investigating the effects of the stimulus source and external load frequencies on the remodelling process demonstrate qualitatively the effectiveness of our approach in predicting the mechanical behaviour of bone tissue. The proposed model offers a promising modelling tool to study the evolution of bone tissue under external mechanical loads. Future work will focus on the extension of our model to incorporate anisotropic material symmetry and the development of techniques to validate the model using experimental data. Furthermore, as damage is a crucial factor in bone remodelling, future advancements will include the impact of damage in the model (see for modelling tools [40–46]).

2. The model

2.1. Mechanical formulation

In this paper, we consider a three-dimensional 3D system composed of trabecular bone tissue characterized by porosity. Generally, bone porosity exhibits various levels at different scales due to multiple distinctive structures, such as inter-trabecular, lacunar-canalicular, and collagen-apatites porosity. Here, we simplify the description to avoid excessive complexity in the model by employing a single scalar variable for modelling the porosity in the framework of generalized continua, as done in Biot [47, 48]. The rationale is to capture the overall behaviour of the tissue even at the expense of a few losses in the detail of the description as a first level of approximation [49].

According to these assumptions, we introduce, as kinematical descriptors, the displacement $\boldsymbol{u}$ of any material particle of the continuum model and the Lagrangian porosity ϕ as follows:

$$\boldsymbol{u} = \boldsymbol{x} - \mathbf{X} \tag{2.1}$$

$$\phi(\mathbf{X}, t) = n[\chi(\mathbf{X}, t)]J(\mathbf{X}, t) \tag{2.2}$$

where $\mathbf{X}$ is any particle of the system in the reference configuration, $\boldsymbol{x} = \chi(\mathbf{X}, t)$ is the position of the particle $\mathbf{X}$ in the current configuration, $n[\chi(\mathbf{X}, t)]$ is the Eulerian porosity and $J = \det(\mathbf{F}) = \det(\nabla\chi(\mathbf{X}, t))$ [50, 51].

It is worth noting that the stiffness of bones has the potential to undergo changes over time, leading to a current configuration that may differ from its initial state. Moreover, since during this evolution, certain regions may experience a massive decrease in stiffness due to an onset of porosity where the material is unneeded, we implement a nonlinear behaviour to cover these compliant areas, as in our previous works [35, 51], assuming that the mechanical response of the bone remains in the elastic domain for the sake of simplicity. Therefore, the assumed measures of deformation, namely, the finite strain tensor $\mathbf{E}_{ij}(\mathbf{X}, t)$ and the change of the Lagrangian porosity $\zeta(\mathbf{X}, t)$ are introduced as:

$$\mathbf{E}_{ij}(\mathbf{X}, t) = \frac{1}{2}(u_{i,j} + u_{j,i} + u_{i,k}u_{k,j}) \tag{2.3}$$

$$\zeta(\mathbf{X}, t) = \phi(\mathbf{X}, t) - \phi^*(\mathbf{X}, t) \tag{2.4}$$

with $\phi(\mathbf{X},t)$ and $\phi^*(\mathbf{X},t)$ the Lagrangian porosities at the current and reference configurations, respectively.

Bone consists of a solid phase and porous space filled with bone marrow, interstitial fluids, blood, and bone cells [37,52,53]. Based on the mixture theory, a representation of $\phi^*(\mathbf{X},t)$ can be introduced as:

$$\phi^*(\mathbf{X},t) = 1 - \frac{\rho^*(\mathbf{X},t)}{\hat{\rho}} \tag{2.5}$$

where the volume fraction of the bone tissue is $\rho^*(\mathbf{X},t)/\hat{\rho}$, being ρ^* the apparent mass density of the bone in the reference configuration and $\hat{\rho}$ the real mass density of the bone without porosity.

To describe the mechanical behaviour of the bone tissue, we postulate a nonlinear energy density $\mathscr{E}$ made of different contributions involving the deformation of the solid phase U_s, the deformation of the pores and thus the change in the fluid content U_f, and the fluid-solid coupling U_{fs} [54] as follows

$$\mathscr{E} = U_s + U_f + U_{fs} = \underbrace{\frac{1}{2}\lambda(\rho^*)E_{ii}E_{jj} + \mu(\rho^*)E_{ij}E_{ji}}_{U_s} + \underbrace{\frac{1}{2}K_1(\rho^*)\zeta^2}_{U_f} + \underbrace{\frac{1}{2}K_2(\rho^*)\left[\zeta - (J-1)\right]^2}_{U_{fs}} \tag{2.6}$$

The behaviour of the solid phase is governed by the Saint-Venant constitutive model for materials with geometrical nonlinearities; the porous deformation is addressed by the standard Biot constitutive model [55, 56], while the exchange of energy between these two deformative modes generalize the standard Biot constitutive model since the energy exchange involves the change of the Lagrange porosity ζ and the nonlinear change of volume $(J-1)$ instead of its linear approximation, namely, the trace of the infinitesimal strain tensor, as done in the original Biot model, which is linear. The material parameters characterizing the model are the Lamé coefficients λ and μ, expressed as

$$\lambda = \frac{\nu\, Y(\rho^*)}{(1+\nu)(1-2\nu)}, \qquad \mu = \frac{Y(\rho^*)}{2\,(1+\nu)} \tag{2.7}$$

in terms of the Young modulus, which depends on bone density, as reported below [57]:

$$Y = Y_{\max}\left(\frac{\rho^*}{\hat{\rho}}\right)^2 \tag{2.8}$$

with $Y_{\max}$ being the maximal bone elastic modulus, i.e., the one related to the mineral part of the tissue without pores, and the Poisson ratio ν, which is kept constant for the sake of simplicity. The coefficients K_1 and K_2 describe the compressibility and the micro-structure, respectively [51]. The coefficient of compressibility, K_1, introduced by Biot [47] can be expressed as:

$$K_1 = \left(\frac{\phi^*}{K_{\mathrm{f}}} + \frac{(\alpha_B - \phi^*)(1-\alpha_B)}{K_{\mathrm{dr}}}\right)^{-1} \tag{2.9}$$

where K_{f} is the stiffness of the fluid filling the pores,

$$K_{\mathrm{dr}} = \frac{Y(\rho^*)}{3\,(1-2\nu)} \tag{2.10}$$

is the drained bulk modulus of the porous matrix, and α_B (satisfying the inequality $\phi^* \leq \alpha_B \leq 1$) is the Biot–Willis coefficient. The micro-structure coupling parameter K_2, which is introduced in the work of Biot [47], can be evaluated as follows:

$$K_2 = \alpha_B\, K_1 \tag{2.11}$$

In the performed numerical simulations, we set

$$\alpha_B = a_1\varphi^* + (1-a_1) \tag{2.12}$$

being $a_1 = 0.8$.

As in our previous works [35, 51], the potential dissipation sources that may be found in the fluid that fills the pores, in the bone solid matrix, or at the interface between the solid and the fluid

phase are integrated through a Rayleigh functional that can be expressed, at a macroscopic level of observation, as

$$2\,\mathscr{D}_s = 2\,\mu^v\left(\dot{E}_{ij}\dot{E}_{ij} - \frac{1}{3}\dot{E}_{ii}\dot{E}_{jj}\right) + k^v\dot{E}_{ii}\dot{E}_{jj} \tag{2.13}$$

where $\dot{E}$ is the solid-matrix rate of deformation and μ^v and k^v are two viscous coefficients related to the deviatoric and hydrodynamic contribution of the deformation, respectively.

In this work, we consider only the remodelling time scale (i.e., order of months) [58]. However, we recognise that the time scale involving mechanical loads (i.e., order of seconds) also plays a critical role [59].

To analyse and obtain the resultant behaviour of the bone tissue subjected to external loads, herein, we employed a generalized version of the principle of virtual work. It provides a powerful tool for solving problems related to mechanical equilibrium and deformations. The principle of virtual work is based on the idea that for a system in equilibrium, the total virtual work done by external and internal forces is zero for any virtual kinematical descriptor; in the examined case, the displacement field and the Lagrangian porosity, compatibly with the constraints of the system. If a dissipative source is significant, we must consider the dissipated energy associated with any virtual kinematical descriptor in the expression of the virtual work. Therefore, the Generalized Principle of Virtual Work that we utilise becomes

$$\int_{\mathscr{B}^*}\delta\mathscr{E}\,d\mathscr{B}^* + \int_{\mathscr{B}^*}\frac{\partial\mathscr{D}_s}{\partial\dot{E}_{ij}}\delta E_{ij}\partial\mathscr{B}^* = \int_{\mathscr{B}^*}\delta\mathscr{W}^{ext}d\mathscr{B}^* \tag{2.14}$$

with $\delta\mathscr{W}^{ext}$ describing the virtual work exerted by external loads, that can be expressed as

$$\delta\mathscr{W}^{ext} = \int_{\partial_\tau\mathscr{B}^*}\tau_i\delta u_i d\mathscr{S}^* \tag{2.15}$$

where this term takes into account the surface forces τ_i on the boundary $\delta_\tau\mathscr{B}^*$ where they are applied. Moreover, since we analyse only the slow time scale characteristic of the remodelling process, the inertial effects are neglected in this work (see for more details [51]).

2.2. Remodelling formulation

Here, we briefly describe the mathematical framework of the remodelling process adopted. The general model is consolidated, albeit referred to as a straightforward formulation involving only the evolution of one material parameter. In particular, we consider the apparent bone mass density (ρ^*) evolution in the reference configuration. This approach fits well the case of an isotropic material symmetry where only two material constants are significant, and in most cases, the variability of the Poisson ratio is negligible. Sometimes, this formulation is too simplistic, and an orthotropic or anisotropic material symmetry is more accurate, but a complete formulation where all the material parameters are involved could be very cumbersome to implement in an efficient model (see, e.g., [31]). Here, we decide to be as simple as possible in addressing the remodelling phenomenon to better understand one aspect of it: specifically, the evolution in time of a material parameter, namely, the Young modulus, which is linked with a phenomenological relationship with the apparent bone mass density (see Eq. (2.8)). Since in a more general model, as done in [31], the single material parameter could grow or decrease with a governing equation which is very similar to the one used herein, it is possible to have significant insight into the evolution of just one parameter with a very simple and effective model without the distraction due to the presence of many parameters and their interplay.

The evolution of the apparent mass density is governed by its time derivative as a function of a mechanical stimulus $S(\mathbf{X},t)$ and the porosity $\phi(\mathbf{X},t)$ as [8, 37, 60–62]

$$\frac{\partial\rho^*}{\partial t}(\mathbf{X},t) = A(S)H(\phi) \quad \text{with} \quad 0 < \rho^* \leq \hat{\rho} \tag{2.16}$$

where A is a piece-wise linear function defined as follows

$$A(S) = \begin{cases} s(S - S_s) & \text{for } (S - S_s) \geq 0 \\ 0 & \text{for } S_r < S < S_s \\ r(S - S_r) & \text{for } (S - S_r) \leq 0 \end{cases} \tag{2.17}$$

where the coefficients s and r are the rates of growth and resorption, respectively, while S_s and S_r are two thresholds that delimit the so-called 'lazy' zone which characterizes the homeostatic state. These two thresholds are evaluated as the energy associated with the deformation of 2000 microstrains and 600 microstrains, respectively (see [5]). The mechanical stimulus is a variable used to catch the fundamental characteristics of the mechanical state of the bone tissue, and Eq. (2.17) represents a control feedback action that aims to restore as much as possible the mechanical state in the reference interval defined by S_r and S_s. The function $H(\phi)$ accounts for the porosity that plays a critical role during the remodelling process. Actually, bone cells can migrate through pores and reach even remote zones of the system to remove or synthesise bone. Two extreme scenarios can be envisaged: i) the porosity is low, cells cannot freely migrate, and bone density does not change, and ii) the porosity is high; thus, there is virtually no bone to be replaced. According to such scenarios, we set the maximal value of H to about 0.55 porosity to provide the most efficient and realistic conditions for bone remodelling to take place (see, for more details, [32]). In other words, the weight function H prevents abnormal cellular activities when porosity is very low or high.

The mechanical stimulus S, in our model, is a result of the sensing capabilities of the osteocytes and induces bone adaptation by the action of osteoclasts and osteoblasts that can modify the bone solid phase and, consequently, its mechanical properties (i.e., the stiffness). This variable S is expressed through a diffusion equation as in [32,35]; in particular, we have:

$$\frac{\partial S}{\partial t} - \kappa \Delta S = f(\rho^*)\, \mathscr{E} - \beta S \tag{2.18}$$

where κ and β are two scalar parameters being the latter activated only when $S > 0$, that is when there is some stimulus. In fact, κ, which is the diffusion coefficient, is responsible for the diffusion of the signal S inside the bone tissue, and β is a sink coefficient that is related to the metabolic absorption of the stimulus once it is generated and diffused. The function $f(\rho^*)$ is a proper signalling weight, a sort of signal efficiency. In fact, the source term for the stimulus has been set to the elastic energy density $\mathscr{E}$, which we assume to be representative of the mechanical state of the bone. We set this function f to be:

$$f(\rho^*) = \frac{1}{2}\left\{ \tanh\left[20\left(\frac{\rho^*}{\hat{\rho}} - 0.15\right)\right] + \tanh\left[20\,(1 - 0.15)\right] \right\} \tag{2.19}$$

This function is monotonically increasing and depends on the apparent mass density of the tissue. We can imagine that osteocytes are distributed almost uniformly in the tissue as the first approximation; hence, their density per unit volume could be assumed to be proportional to the volume fraction. Moreover, the more the osteocytes are, the more their capability to 'sense' the mechanical state of the bone is better; thus, we set this monotonic trend for f, and when the volume fraction is near 0.5, we have the maximum efficiency of the osteocytes as we can deduce from the more efficient activity of the osteoblast and osteoclast in that condition as derives from the values of H.

The initial value of S in the bone is set to be equal to 4.275×10^{-9}, corresponding to homeostasis. Regarding the boundary conditions, we set Neumann ones, assuming no stimulus flux is exchanged with the outside.

3. Numerical simulations of a 3D illustrative case

In this section, we employ the proposed model to evaluate its predictive abilities through a finite element formulation. It is worth noting that the ability of this model to predict the outcome of bone evolution is of particular interest in its potential applicability in real-world scenarios as well as many

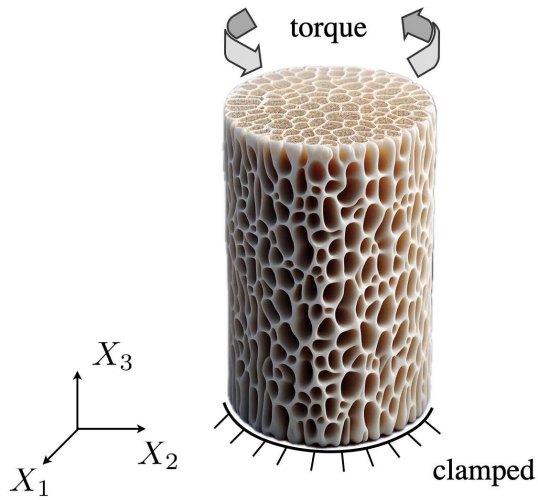

FIGURE 1. Schematic representation of the 3D system under study. The cylindrical sample is constituted only by isotropic bone tissue. It is subjected to a dynamic cyclic torsion on the upper surface and the displacements are fully constrained on the bottom surface.

medical applications. The finite element formulation provides a robust framework for this purpose, which facilitates accurately evaluating the model performance. Specifically, we consider a simplified cylindrical specimen with a length of 15 cm and a radius of 2 cm, representative of a femoral diaphysis in an academic example (see Fig. 1 for a visual representation of the setup). The specimen is solely composed of bone tissue, with an initial apparent bone mass density ρ^* uniformly distributed. A reference frame is introduced with the X_3-axis aligned with the axis of the cylinder and having the origin coinciding with the centre of the bottom circular base of the specimen. The components of the displacement of the cylinder bottom surface are fully constrained, while on the top surface, a sinusoidal force per unit surface $\boldsymbol{\tau}(X_1, X_2, t)$ which produces a twisting deformation, is applied as follows

$$\boldsymbol{\tau}(X_1, X_2, t) = A_0(X_2\,\mathbf{e}_1 - X_1\,\mathbf{e}_2)\sin(2\pi\,\Omega\,t) \tag{3.1}$$

where A_0 is a nominal amplitude for the distribution of force applied and Ω is the frequency. The lateral surface is free from any mechanical load. The model parameters used in the numerical analysis are reported in Table 1.

In this paper, we employed COMSOL Multiphysics software to conduct the numerical investigation. The partial differential equations constituting the proposed model previously delineated are directly solved with a weak formulation that implements the finite element analysis. The simulation results were obtained through a parametric analysis of the most important parameters characteristic of the adopted model: the frequency of the external load and the sink coefficient β.

4. Results and discussion

In order to scrutinize the numerical results, two probe points located within the cylinder have been considered. The first point, denoted as point 1, is situated in the centre of the specimen $(0, 0, 7.5)$ cm, while the second point, denoted as point 2, is located on the lateral surface of the cylinder, precisely at $(2, 0, 7.5)$ cm.

We have performed two distinct sets of simulations aiming to evaluate the impact of the frequency Ω (Fig. 2) and coefficient β (Fig. 5) on: 1) the stimulus S, 2) the apparent mass density ρ^*, and 3) the bone elastic modulus Y. Our findings provide crucial insights into how these variables interplay

L (cm)	15
r (cm)	2
$\hat{\rho}$ (kg/m^3)	1800
ν	0.3
$Y_{\max}$ (GPa)	17
ν^v (N s/m^2)	2.57x10^{12}
k^v (N s/m^2)	2.06x10^{12}
s (s/m^2)	1.27x10^{-7}
r (s/m^2)	1.06x10^{-7}
S_s (J)	848.23
S_r (J)	254.47
κ (m^2/s)	1.6x10^{-4}
β	0.6
ψ (N)	1.68x10^{-3}
A_0 (MPa/m)	200

TABLE 1. Material parameters used in the numerical analysis.

and affect the overall outcome. These results hold significant value and can help in advancing the knowledge of the field. In the former case, we have let the frequency vary between $\Omega = 0.01$ cycles per reference time (CpT), 0.1 CpT, and 1 CpT, and we have set $\beta = 0.1$. In the latter case, β takes the values of 0.01, 0.1 and 1 while $\Omega = 1$ CpT. It has been established that the reference time t_{ref} is equivalent to one week, which amounts to 604800 seconds. This characteristic time for the bone remodelling process has been put in place to ensure consistency and accuracy in our simulations, which examine the behaviour of the bone tissue at a slow time scale. Indeed, the standard period of time for an entire cycle of mass turnover in trabecular bone is about 120 days [58]. Therefore, a unit time of 1 week is a sufficiently small unit of time that is simultaneously accurate and still saves computing power.

Analysing the variability in the outcome of the remodelling process due to the frequency of the external torque applied to the sample (Fig. 2), we observe from the panels (A), (B), and (C) that the level of the stimulus S produced from the external mechanical stimulation changes with the frequency. More precisely, we remark that the average trend of the stimulus is the same, especially for point 2 (see, for comparison, Fig. 3). However, the local slope varies significantly due to the actual frequency. Therefore, the transient behaviour turns out to be quite different. Indeed, the lower the frequency, the more delay appears in the onset in the initial slope. On the contrary, as the frequency increases, the general behaviour tends to be asymptotically the same. As the frequency increases at point 2, the stimulus has a more extensive boost during the initial stage due to the average trend, while in the middle of the specimen (point 1), we notice little resorption or no evolution in all the cases. The disparity in the spatial behaviour of the sample can be attributed to the distribution of energy density within. In the twisting case analysed, it is common knowledge that the deformation energy tends to localize at the lateral surface, while it is nearly negligible at the sample centre. To illustrate this distribution, in Fig. 4, the evolution of the stimulus S over time is reported in the entire 3D sample for the configuration defined by $\Omega = 1$ and two values of β, 0.1 (see first row of Fig. 4, corresponding

to Fig. 2(C)) and 1 (see second row of Fig. 4, corresponding to Fig. 5(C)). One can observe that the stimulus increases on the periphery of the sample, whereas it stays very close to its initial value inside. Furthermore, the asymptotic behaviour observed in Fig. 2 (A:C) implies that over a certain frequency, if the stimulus source is the energy density, the dependence of the bone evolution on time due to time-variable loads becomes inconsequential; thus, the influence of the external dynamic stimulation is valid but in a suitable range of frequencies where the transient behaviour occurs in a period comparable with the cycle of remodelling, namely 120 days.

The second row of panels of Fig. 2, from (D) to (F), exhibits the trend of the apparent mass density ρ^*. At point 1, for all the examined cases where the stimulus has a little drop, the mass density is relatively unaffected, being the stimulus in the so-called range 'lazy zone', characteristic of the homeostatic state. However, in point 2, depending on the level of stimulus reached, we note that for the low frequency, $\Omega = 0.01$ CpT, the mass density has no significant alteration for a longer period; while increasing the load frequency, the production of new bone tissue is promoted earlier. Moreover, since the average stimulus is the same, we note that the rate of growth is the same for the mass density even though, at the same instant, the level of mass density is different for the delay in commencing the synthesis of new bone.

The panels of Fig. 2, from (G) to (I), show the elastic modulus Y. Because it is related to the bone mass density by means of the monotonic relationship (2.8), these panels are characterized by the same trend as the previous row for the mass density.

Figure 5 shows the influence of the parameter β, which takes the values $\{0.01, 0.1, 1\}$, in the bone evolution. We note from the panels (A), (B), and (C) that the level of the stimulus S tends to have lower levels as the sink coefficient β grows. The same trend is observed in both probe points; due to the small scale of the stimulus at point 1, in Fig. 6, the plot of the stimulus has been zoomed in for clarity. The effect of these changes has a larger impact on the central zone, i.e., point 1. In this region, there is a certain amount of stimulus due to the diffusion but it disappears faster as the β coefficient increases. Thus, we note the most significant resorption in panel (F) related to the biggest value of β tested. In the other two cases at point 1, we have almost the same behaviour with a sudden drop at the end of the simulation for the smallest value of β. This effect is difficult to explain since it results from different effects that play a role in it, such as the speed in the diffusion of the stimulus and the overall value of the stimulus. Regarding point 2, we have almost no change in the bone production, just a slight perceptible delay at the beginning of the process in the last case, namely, $\beta = 1$. Once again, this odd behaviour is the combination of different factors acting simultaneously; thus, it is not an easy task to understand the reason beyond it. Finally, the evolution of the Young modulus is depicted in the panels from (G) to (I). The qualitative behaviour of it matches with the one of the mass density, as expected.

In summary, the present contribution aims to model the mechanical behaviour of bone tissue employing a generalized three-dimensional deformable continuum, which takes into account the porous nature of the tissue with a nonlinear constitutive law. In this work, indeed, we generalize some results from previous works, where we applied the mathematical model to two-dimensional (2D) geometries constituted by bone and graft region [35, 51]. To simplify the problem, we have adopted an isotropic material symmetry, focusing on the interplay between the tissue evolution and the stimulus model. This formulation shows promise, as it allows the bone tissue to evolve based on the time-variability of external mechanical loads, even if the source of the stimulus is assumed to be the strain energy density, which is notoriously not rate-dependent. Therefore, unlike other similar models for the stimulus (see [37]), the fundamental effects of dynamic loads on the remodelling process can be taken into account because of the time dependency introduced by the diffusive nature attributed to the stimulus due to the transient behaviour. However, this dependence is characteristic of only a range of frequencies; beyond a certain threshold, it disappears. This behaviour is not in contradiction with the clinic experience. In the rehabilitative treatments, only a few specific frequencies seem to be optimal for bone production. Hence, it is worth investigating this aspect more together with introducing dissipative energy as a

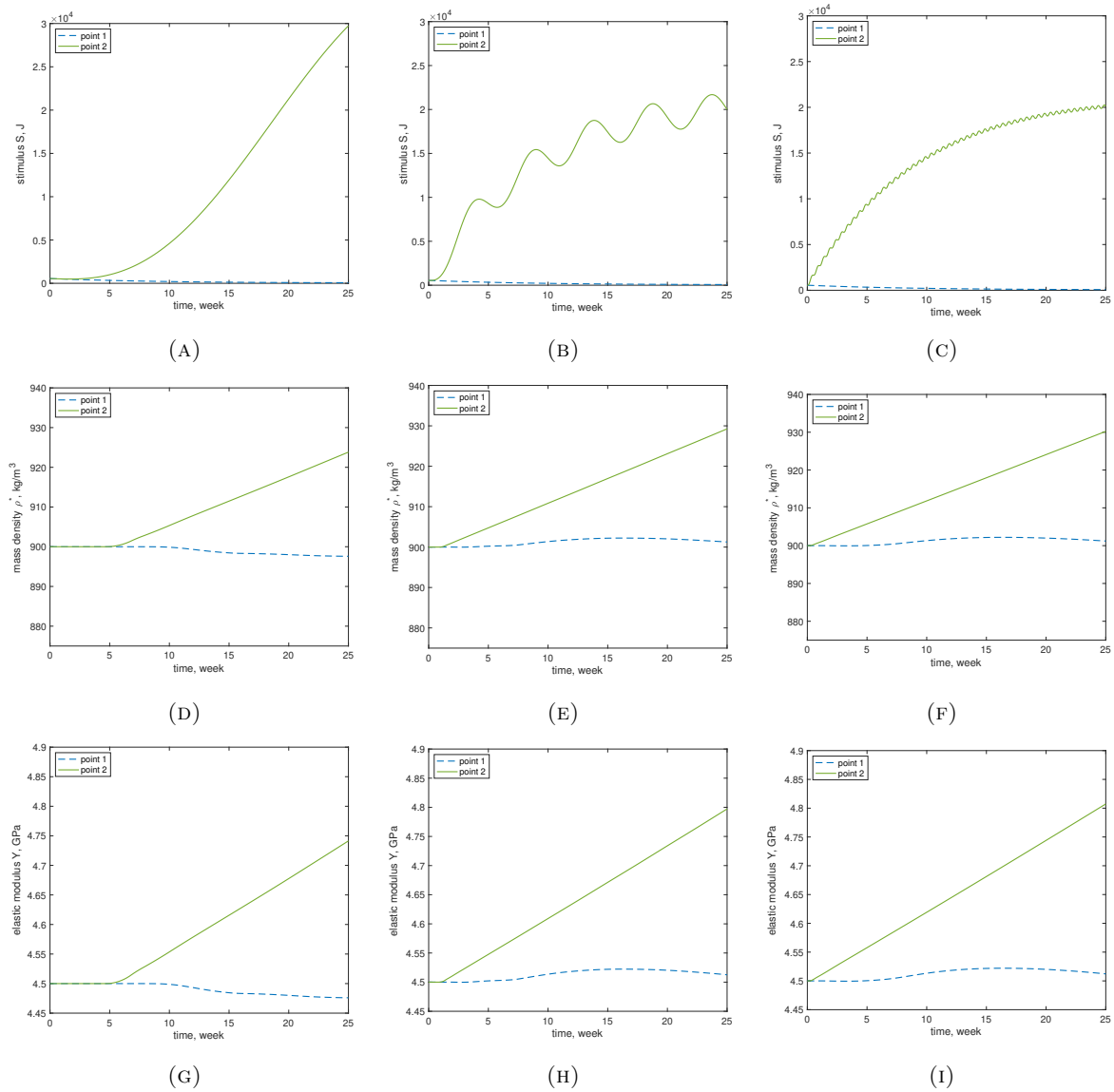

FIGURE 2. Influence of the frequency Ω on the stimulus S (A:C), the apparent mass density ρ^* (D:F) and the bone elastic modulus Y (G:I) for point 1 (dashed blue line) and point 2 (solid green line). $\beta = 0.1$ and $\Omega = 0.01$ CpT (A,D,G), $\Omega = 0.1$ CpT (B,E,H) and $\Omega = 1$ CpT (C,F,I).

co-source of the stimulus to have a more comprehensive dependence on the time variability of the load.

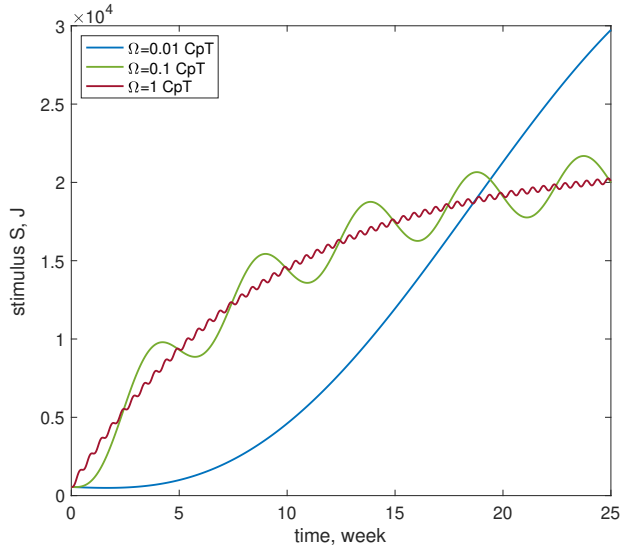

FIGURE 3. Time history of the stimulus S at point 2 for the different frequencies Ω evaluated and $\beta = 0.1$.

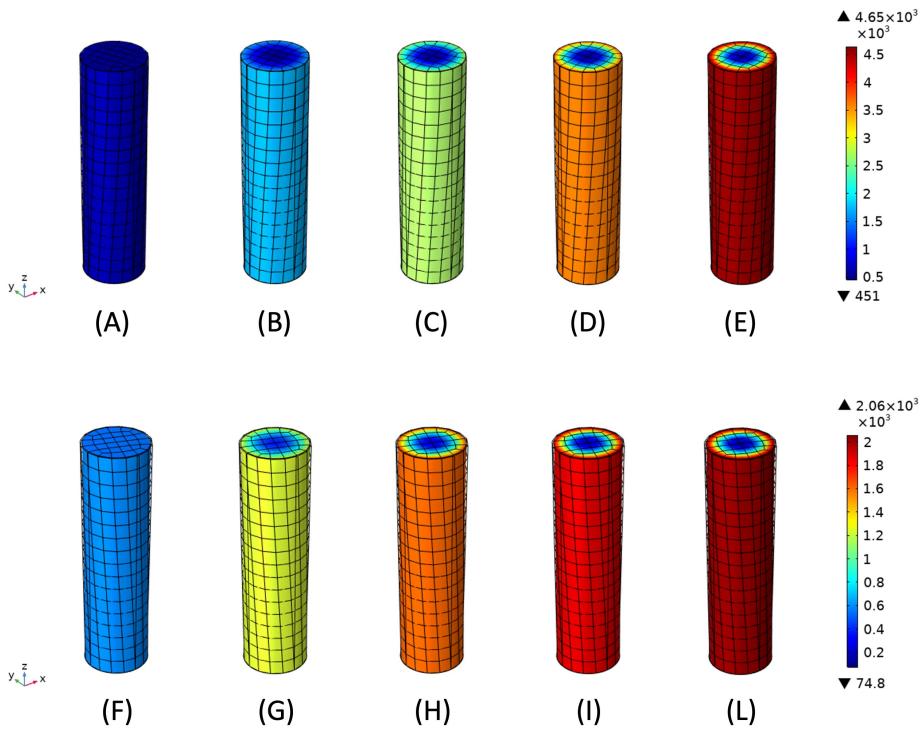

FIGURE 4. Evolution over time of the stimulus S for the configurations defined by $\Omega = 1$ and $\beta = 0.1$ (A:E) and $\Omega = 1$ and $\beta = 1$ (F:L).

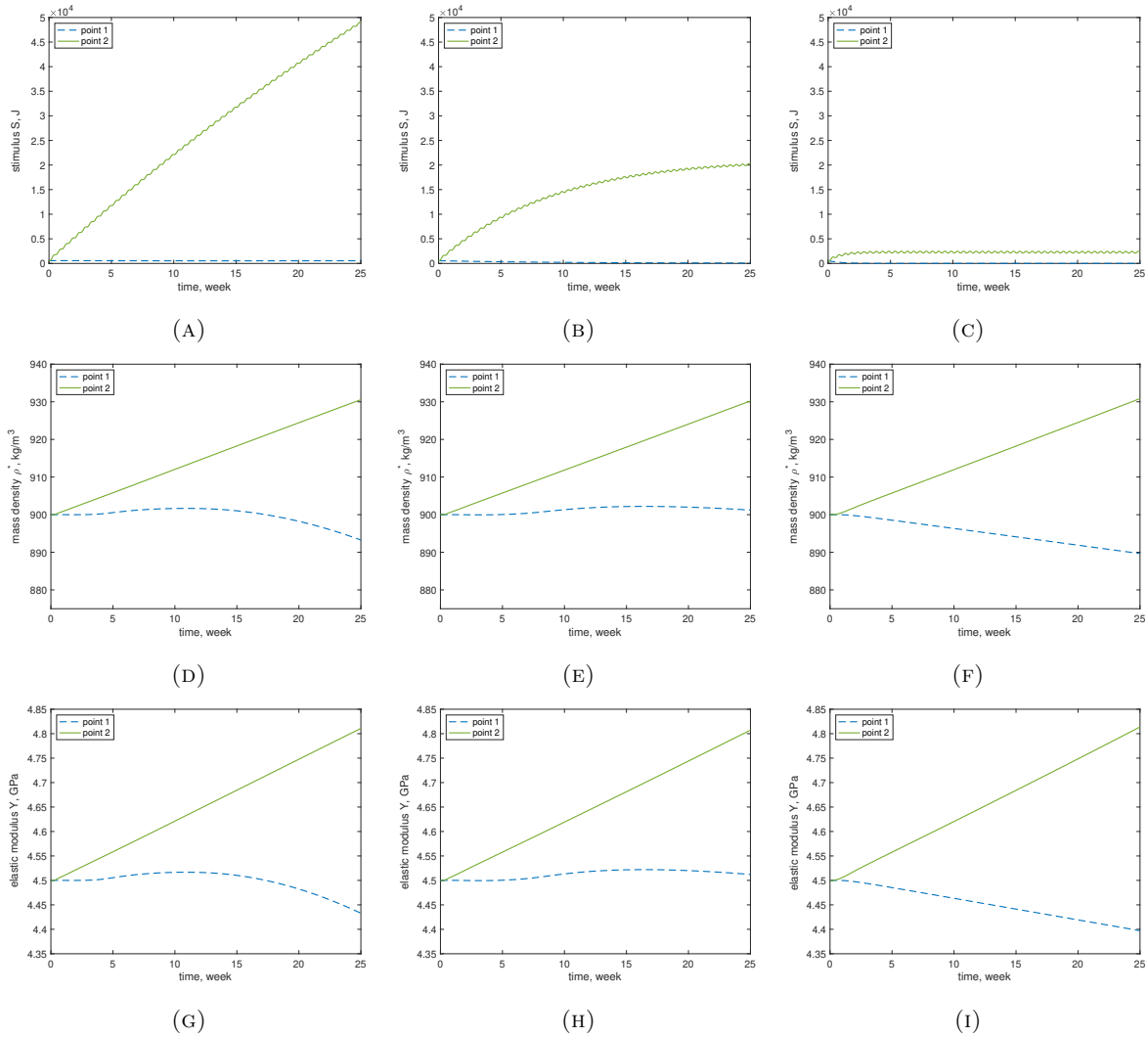

FIGURE 5. Influence of the coefficient β on the stimulus S (A:C), the apparent mass density ρ^* (D:F) and the bone elastic modulus Y (G:I) for point 1 (dashed blue line) and point 2 (solid green line). $\Omega = 1$ CpT and $\beta = 0.01$ (A,D,G), $\beta = 0.1$ (B,E,H) and $\beta = 1$ (C,F,I).

Acknowledgment

This work was carried out under the auspices of the Gruppo Nazionale di Fisica Matematica (GNFM) of the Istituto Nazionale di Alta Matematica (INDAM).

Declarations

Ethical Approval: Not applicable.
Funding: No specific funding was allocated for the present study.
Availability of data and materials: Not applicable.

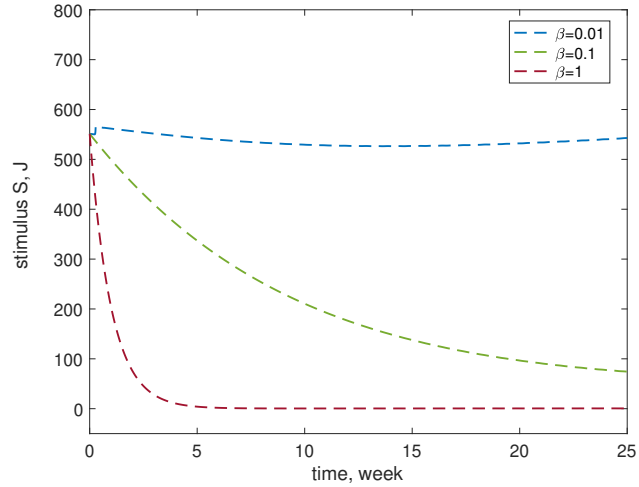

FIGURE 6. Time history of the stimulus S at point 1, zoom for the different sink coefficients β evaluated and $\Omega = 1$.

References

[1] J.-F. Ganghoffer, "A contribution to the mechanics and thermodynamics of surface growth. application to bone external remodeling," *International Journal of Engineering Science*, vol. 50, no. 1, pp. 166–191, 2012.

[2] G. Holzapfel and R. Ogden, *Mechanics of Biological Tissue*. Springer Berlin Heidelberg, 2010.

[3] Y.-F. Hsieh and C. H. Turner, "Effects of loading frequency on mechanically induced bone formation," *Journal of Bone and Mineral Research*, vol. 16, no. 5, pp. 918–924, 2001.

[4] C. H. Turner, "Three rules for bone adaptation to mechanical stimuli," *Bone*, vol. 23, no. 5, pp. 399–407, 1998.

[5] C. T. Rubin and L. E. Lanyon, "Osteoregulatory nature of mechanical stimuli: function as a determinant for adaptive remodeling in bone," *Journal of orthopaedic research*, vol. 5, no. 2, pp. 300–310, 1987.

[6] L. E. Lanyon and C. Rubin, "Static vs dynamic loads as an influence on bone remodelling," *Journal of biomechanics*, vol. 17, no. 12, pp. 897–905, 1984.

[7] D. George, R. Allena, and Y. Rémond, "Mechanobiological stimuli for bone remodeling: mechanical energy, cell nutriments and mobility," *Computer Methods in Biomechanics and Biomedical Engineering*, vol. 20, no. sup1, pp. S91–S92, 2017. PMID: 29088669.

[8] D. George, R. Allena, and Y. Remond, "A multiphysics stimulus for continuum mechanics bone remodeling," *Math. Mech. Complex Syst.*, vol. 6, no. 4, pp. 307–319, 2018.

[9] D. George, R. Allena, and Y. Rémond, "Integrating molecular and cellular kinetics into a coupled continuum mechanobiological stimulus for bone reconstruction," *Continuum Mechanics and Thermodynamics*, vol. 31, pp. 725–740, May 2019.

[10] I. Goda, M. Assidi, and J.-F. Ganghoffer, "A 3D elastic micropolar model of vertebral trabecular bone from lattice homogenization of the bone microstructure," *Biomechanics and modeling in mechanobiology*, vol. 13, pp. 53–83, 2014.

[11] I. Giorgio, U. Andreaus, F. Dell'Isola, and T. Lekszycki, "Viscous second gradient porous materials for bones reconstructed with bio-resorbable grafts," *Extreme Mechanics Letters*, vol. 13, pp. 141–147, 2017.

[12] A. Madeo, D. George, T. Lekszycki, M. Nierenberger, and Y. Rémond, "A second gradient continuum model accounting for some effects of micro-structure on reconstructed bone remodelling," *Comptes Rendus Mécanique*, vol. 340, no. 8, pp. 575–589, 2012.

[13] V. Eremeyev, A. Skrzat, and A. Vinakurava, "Application of the micropolar theory to the strength analysis of bioceramic materials for bone reconstruction," *Strength of Materials*, vol. 48, pp. 573–582, 2016.

[14] L. You, S. C. Cowin, M. B. Schaffler, and S. Weinbaum, "A model for strain amplification in the actin cytoskeleton of osteocytes due to fluid drag on pericellular matrix," *Journal of Biomechanics*, vol. 34, no. 11, pp. 1375–1386, 2001.

[15] R. Rieger, R. Hambli, and R. Jennane, "Modeling of biological doses and mechanical effects on bone transduction," *Journal of theoretical biology*, vol. 274, no. 1, pp. 36–42, 2011.

[16] M. Kühl, L. C. Sheldahl, M. Park, J. R. Miller, and R. T. Moon, "The Wnt/Ca2+ pathway: a new vertebrate Wnt signaling pathway takes shape," *Trends in genetics*, vol. 16, no. 7, pp. 279–283, 2000.

[17] K. I. Pinson, J. Brennan, S. J. Monkley, B. J. Avery, and W. C. Skarnes, "An ldl-receptor-related protein mediates wnt signalling in mice," *Nature*, vol. 407, pp. 535–538, 2000.

[18] N. Branecka, M. E. Yildizdag, A. Ciallella, and I. Giorgio, "Bone remodeling process based on hydrostatic and deviatoric strain mechano-sensing," *Biomimetics*, vol. 7, no. 2, p. 59, 2022.

[19] A. M. Bersani and G. Dell'Acqua, "Is there anything left to say on enzyme kinetic constants and quasi-steady state approximation?," *J. Math. Chem.*, vol. 50, no. 2, pp. 335–344, 2012.

[20] D. George, R. Allena, C. Bourzac, S. Pallu, M. Bensidhoum, H. Portier, and Y. Rémond, "A new comprehensive approach for bone remodeling under medium and high mechanical load based on cellular activity," *Math. Mech. Complex Syst.*, vol. 8, no. 4, pp. 287–306, 2020.

[21] A. Grillo and S. Di Stefano, "A formulation of volumetric growth as a mechanical problem subjected to non-holonomic and rheonomic constraint," *Mathematics and Mechanics of Solids*, vol. 28, pp. 2215–2241, 2023.

[22] A. Grillo, G. Wittum, A. Tomic, and S. Federico, "Remodelling in statistically oriented fibre-reinforced materials and biological tissues," *Mathematics and Mechanics of Solids*, vol. 20, no. 9, pp. 1107–1129, 2015.

[23] A. Misra, L. Placidi, F. dell'Isola, and E. Barchiesi, "Identification of a geometrically nonlinear micromorphic continuum via granular micromechanics," *Zeitschrift für angewandte Mathematik und Physik*, vol. 72, pp. 1–21, 2021.

[24] L. Placidi, E. Barchiesi, F. dell'Isola, V. Maksimov, A. Misra, N. Rezaei, A. Scrofani, and D. Timofeev, "On a hemi-variational formulation for a 2D elasto-plastic-damage strain gradient solid with granular microstructure," *Mathematics in Engineering*, vol. 5, pp. 1–24, 2022.

[25] L. Placidi, D. Timofeev, V. Maksimov, E. Barchiesi, A. Ciallella, A. Misra, and F. dell'Isola, "Micro-mechano-morphology-informed continuum damage modeling with intrinsic 2nd gradient (pantographic) grain–grain interactions," *International Journal of Solids and Structures*, vol. 254, p. 111880, 2022.

[26] L. Placidi, F. dell'Isola, N. Ianiro, and G. Sciarra, "Variational formulation of pre-stressed solid–fluid mixture theory, with an application to wave phenomena," *European Journal of Mechanics-A/Solids*, vol. 27, no. 4, pp. 582–606, 2008.

[27] S. Massoumi and G. La Valle, "Static analysis of 2D micropolar model for describing granular media by considering relative rotations," *Mechanics Research Communications*, vol. 119, p. 103812, 2022.

[28] G. La Valle, B. E. Abali, G. Falsone, and C. Soize, "Sensitivity of a homogeneous and isotropic second-gradient continuum model for particle-based materials with respect to uncertainties," *ZAMM-Journal of Applied Mathematics and Mechanics/Zeitschrift für Angewandte Mathematik und Mechanik*, p. e202300068, 2023.

[29] M. Laudato and M. Mihaescu, "Analysis of the contact critical pressure of collapsible tubes for biomedical applications," *Continuum Mechanics and Thermodynamics*, pp. 1–12, 2023.

[30] G. La Valle, "A new deformation measure for the nonlinear micropolar continuum," *Zeitschrift für angewandte Mathematik und Physik*, vol. 73, no. 2, p. 78, 2022.

[31] I. Giorgio, F. dell'Isola, U. Andreaus, and A. Misra, "An orthotropic continuum model with substructure evolution for describing bone remodeling: an interpretation of the primary mechanism behind Wolff's law," *Biomechanics and Modeling in Mechanobiology*, vol. 22, no. 6, pp. 2135–2152, 2023.

[32] I. Giorgio, F. dell'Isola, U. Andreaus, F. Alzahrani, T. Hayat, and T. Lekszycki, "On mechanically driven biological stimulus for bone remodeling as a diffusive phenomenon," *Biomech. Model. Mechanobiol*, vol. 18, no. 6, pp. 1639–1663, 2019.

[33] I. Giorgio, U. Andreaus, F. dell'Isola, and T. Lekszycki, "Viscous second gradient porous materials for bones reconstructed with bio-resorbable grafts," *Extreme Mechanics Letters*, vol. 13, pp. 141–147, 2017.

[34] I. Giorgio, U. Andreaus, D. Scerrato, and F. dell'Isola, "A visco-poroelastic model of functional adaptation in bones reconstructed with bio-resorbable materials," *Biomechanics and modeling in mechanobiology*, vol. 15, no. 5, pp. 1325–1343, 2016.

[35] R. Allena, D. Scerrato, A. Bersani, and I. Giorgio, "A model for the bio-mechanical stimulus in bone remodelling as a diffusive signalling agent for bones reconstructed with bio-resorbable grafts," *Mechanics Research Communications*, vol. 129, p. 104094, 2023.

[36] D. Scerrato, I. Giorgio, A. M. Bersani, and D. Andreucci, "A proposal for a novel formulation based on the hyperbolic Cattaneo's equation to describe the mechano-transduction process occurring in bone remodeling," *Symmetry*, vol. 14, no. 11, p. 2436, 2022.

[37] T. Lekszycki and F. dell'Isola, "A mixture model with evolving mass densities for describing synthesis and resorption phenomena in bones reconstructed with bio-resorbable materials," *ZAMM - Z. Angew. Math. Mech*, vol. 92, no. 6, pp. 426–444, 2012.

[38] M. Mullender and R. Huiskes, "Proposal for the regulatory mechanism of Wolff's law," *Journal of orthopaedic research*, vol. 13, no. 4, pp. 503–512, 1995.

[39] I. Giorgio, U. Andreaus, D. Scerrato, and P. Braidotti, "Modeling of a non-local stimulus for bone remodeling process under cyclic load: Application to a dental implant using a bioresorbable porous material," *Mathematics and Mechanics of Solids*, vol. 22, no. 9, pp. 1790–1805, 2017.

[40] L. Placidi, E. Barchiesi, and A. Misra, "A strain gradient variational approach to damage: a comparison with damage gradient models and numerical results," *Mathematics and Mechanics of Complex Systems*, vol. 6, no. 2, pp. 77–100, 2018.

[41] B. E. Abali, A. Klunker, E. Barchiesi, and L. Placidi, "A novel phase-field approach to brittle damage mechanics of gradient metamaterials combining action formalism and history variable," 2021.

[42] B. Vazic, B. E. Abali, H. Yang, and P. Newell, "Mechanical analysis of heterogeneous materials with higher-order parameters," *Engineering with Computers*, pp. 1–17, 2021.

[43] M. Cuomo, L. Contrafatto, and L. Greco, "A variational model based on isogeometric interpolation for the analysis of cracked bodies," *International Journal of Engineering Science*, vol. 80, pp. 173–188, 2014.

[44] A. Battista, L. Rosa, R. dell'Erba, and L. Greco, "Numerical investigation of a particle system compared with first and second gradient continua: Deformation and fracture phenomena," *Mathematics and Mechanics of Solids*, vol. 22, no. 11, pp. 2120–2134, 2017.

[45] M. Spagnuolo, M. E. Yildizdag, X. Pinelli, A. Cazzani, and F. Hild, "Out-of-plane deformation reduction via inelastic hinges in fibrous metamaterials and simplified damage approach," *Mathematics and Mechanics of Solids*, vol. 27, no. 6, pp. 1011–1031, 2022.

[46] M. Valmalle, A. Vintache, B. Smaniotto, F. Gutmann, M. Spagnuolo, A. Ciallella, and F. Hild, "Local–global dvc analyses confirm theoretical predictions for deformation and damage onset in torsion of pantographic metamaterial," *Mechanics of Materials*, vol. 172, p. 104379, 2022.

[47] M. A. Biot, "Mechanics of deformation and acoustic propagation in porous media," *J. Appl. Phys.*, vol. 33, no. 4, pp. 1482–1498, 1962.

[48] M. A. Biot, "Generalized theory of acoustic propagation in porous dissipative media," *The Journal of the Acoustical Society of America*, vol. 34, no. 9A, pp. 1254–1264, 1962.

[49] S. C. Cowin, "Bone poroelasticity," *J. Biomech.*, vol. 32, no. 3, pp. 217–238, 1999.

[50] O. Coussy, *Poromechanics*. John Wiley & Sons, 2004.

[51] D. Scerrato, A. M. Bersani, and I. Giorgio, "Bio-inspired design of a porous resorbable scaffold for bone reconstruction: A preliminary study," *Biomimetics*, vol. 6, no. 1, 2021.

[52] Y. Lu and T. Lekszycki, "Modelling of bone fracture healing: influence of gap size and angiogenesis into bioresorbable bone substitute," *Math. Mech. Solids.*, vol. 22, no. 10, pp. 1997–2010, 2017.

[53] E. Bednarczyk and T. Lekszycki, "A novel mathematical model for growth of capillaries and nutrient supply with application to prediction of osteophyte onset," *ZAMP - Z. fur Angew. Math. Phys*, vol. 67, no. 4, pp. 1–14, 2016.

[54] I. Giorgio, M. De Angelo, E. Turco, and A. Misra, "A Biot–Cosserat two-dimensional elastic nonlinear model for a micromorphic medium," *Continuum Mechanics and Thermodynamics*, vol. 32, no. 5, pp. 1357–1369, 2020.

[55] M. A. Biot, "Mechanics of deformation and acoustic propagation in porous media," *Journal of applied physics*, vol. 33, no. 4, pp. 1482–1498, 1962.

[56] S. C. Cowin and J. W. Nunziato, "Linear elastic materials with voids," *J. Elast.*, vol. 13, no. 2, pp. 125–147, 1983.

[57] J. D. Currey, "The effect of porosity and mineral content on the Young's modulus of elasticity of compact bone," *Journal of biomechanics*, vol. 21, no. 2, pp. 131–139, 1988.

[58] E. F. Eriksen, "Cellular mechanisms of bone remodeling," *Rev. Endocr. Metab. Disord.*, vol. 11, no. 4, pp. 219–227, 2010.

[59] P. Heinemann and M. Kasperski, "Damping induced by walking and running," *Procedia Eng.*, vol. 199, pp. 2826–2831, 2017.

[60] G. Beaupré, T. Orr, and D. Carter, "An approach for time-dependent bone modeling and remodeling–theoretical development," *J. Orthop. Res.*, vol. 8, no. 5, pp. 651–661, 1990.

[61] E. Barchiesi and N. Hamila, "Maximum mechano-damage power release-based phase-field modeling of mass diffusion in damaging deformable solids," *Zeitschrift für angewandte Mathematik und Physik*, vol. 73, no. 1, p. 35, 2022.

[62] E. Bednarczyk, S. Sikora, K. Jankowski, Z. Żołek-Tryznowska, T. Murawski, J. Bańczerowski, Y. Lu, and C. Senderowski, "Mathematical model of osteophyte development with the first attempt to identify a biomechanical parameter," *Continuum Mechanics and Thermodynamics*, 2024.

Rachele Allena
Laboratoire Jean Alexandre Dieudonnè UMR CNRS
Université Côte d'Azur
Nice
France
e-mail: `rachele.allena@unice.fr`

Daria Scerrato
DIMA - Department of Mechanical and Aerospace Engineering
University of Rome La Sapienza
Rome
Italy
e-mail: `daria.scerrato@uniroma1.it`

Alberto M. Bersani
DIMA - Department of Mechanical and Aerospace Engineering
University of Rome La Sapienza
Rome
Italy
e-mail: `alberto.bersani@uniroma1.it`

Ivan Giorgio
DICEAA - Department of Civil, Construction-Architectural and Environmental Engineering
University of L'Aquila
L'Aquila
Italy
e-mail: `ivan.giorgio@univaq.it`